

Experimental Observation of the Bogoliubov Transformation for a Bose-Einstein Condensed Gas

J. M. Vogels, K. Xu, C. Raman,* J. R. Abo-Shaeer, and W. Ketterle†

Department of Physics, MIT-Harvard Center for Ultracold Atoms, and Research Laboratory of Electronics, Massachusetts Institute of Technology, Cambridge, Massachusetts 02139

(Received 11 September 2001; published 28 January 2002)

Phonons with wave vector q/\hbar were optically imprinted into a Bose-Einstein condensate. Their momentum distribution was analyzed using Bragg spectroscopy with a high momentum transfer. The wave function of the phonons was shown to be a superposition of $+q$ and $-q$ free particle momentum states, in agreement with the Bogoliubov quasiparticle picture.

DOI: 10.1103/PhysRevLett.88.060402

PACS numbers: 05.30.Jp, 03.75.Fi, 32.80.-t, 67.40.Db

The pioneering work of Bogoliubov in 1947 constitutes the first microscopic theory that attributes superfluidity to Bose-Einstein condensation [1]. As described by Einstein, noninteracting bosons condense [2], but they are not superfluid. However, Bogoliubov showed that with weak interactions the condensate will exhibit superfluidity. Repulsive interactions change the elementary excitations at long wavelengths from free particles into phonons which, according to the Landau criterion, lead to superfluidity [3]. The main step in the nonperturbative treatment is the Bogoliubov transformation

$$\begin{aligned} b_{+q}^\dagger &:= u_q a_{+q}^\dagger + v_q a_{-q}, \\ b_{+q} &:= u_q a_{+q} + v_q a_{-q}^\dagger, \end{aligned} \quad (1)$$

which expresses the creation and annihilation operators b_q^\dagger and b_q for Bogoliubov quasiparticles in terms of creation and annihilation operators a_q^\dagger and a_q for free particles in momentum states q . This transformation also plays a crucial role in general relativity, where it connects the particle operators in different reference frames [4]. In this paper we experimentally verify the Bogoliubov transformation by generating quasiparticles with momentum $+q$ and observing that they are a superposition of $+q$ and $-q$ momentum states of free particles.

Following a recent suggestion of Brunello *et al.* [5], we perform an experiment that combines the two regimes of Bragg spectroscopy, where the momentum imparted to the atoms is either smaller [6] or larger [7] than the sound velocity c times the mass m of the atoms. An optical lattice moving through the condensate at the sound velocity imprinted phonons with wavelengths equal to the spatial period of the lattice [6]. This was accomplished by intersecting two laser beams at a small angle and choosing their frequency difference to be equal to the phonon frequency. The momentum analysis of the phonon wave function was performed by a second Bragg pulse consisting of counterpropagating laser beams that transferred a large momentum Q (two photon recoils) to atoms with initial momentum p . In the limit $Q \gg p, mc$, the resonance frequency ν is equal to the kinetic energy

transferred: $h\nu = Q^2/2m + Qp/m$, where the second term is simply the Doppler shift [7–9]. The resulting frequency spectrum shows three peaks corresponding to the three momentum components (0 , $+q$, and $-q$) of a condensate with phonons (see Fig. 2 below) [5].

The Bogoliubov spectrum for the energy of elementary excitations is [10]

$$\varepsilon(q) = \sqrt{q^2 c^2 + \left(\frac{q^2}{2m}\right)^2}, \quad (2)$$

where $c = \sqrt{4\pi\hbar^2 a n}/m$, a is the scattering length, and n is the density. The amplitudes u_q and v_q in Eq. (1) are given by

$$u_q, v_q = \pm \frac{\varepsilon(q) \pm \frac{q^2}{2m}}{2\sqrt{\varepsilon(q) \frac{q^2}{2m}}}. \quad (3)$$

The nontrivial aspect of the Bogoliubov transformation manifests itself only at low momenta ($q \ll mc$), where both amplitudes u_q and v_q are significant. In this regime, the excitations are characterized by $u \sim -v \sim \sqrt{mc/2q} \gg 1$ and $\varepsilon(q) \sim qc$. Such excitations are phonons, each involving many particles moving in both directions. At high momenta ($q \gg mc$), $u_q \sim 1$, $v_q \sim 0$, and $\varepsilon(q) = q^2/2m + mc^2$. These excitations are free particles with an energy shift equal to the chemical potential $\mu = mc^2$.

The phonon creation operator b_{+q}^\dagger [Eq. (1)] is a superposition of the creation operator a_{+q}^\dagger for particles moving in the $+q$ direction and the annihilation operator a_{-q} for particles moving in the $-q$ direction, yet the creation of a phonon in the condensate implies an increase of particles moving in both the $+q$ and $-q$ direction. Indeed, simple operator algebra shows that a condensate with l excitations, $b_{+q}^\dagger/\sqrt{l!}|\Psi_0\rangle$, contains $lu_q^2 + v_q^2$ free particles moving with momentum $+q$ and $(l+1)v_q^2$ free particles with momentum $-q$. In its ground state the condensate contains v_q^2 pairs of atoms with momenta $+q$ and $-q$. These pairs constitute the quantum depletion in the condensate wave function [10]

$$|\Psi_0\rangle = \prod_{q \neq 0} \frac{1}{u_q} \sum_{j=0}^{\infty} \left(-\frac{v_q}{u_q} \right)^j |n_{-q} = j, n_{+q} = j\rangle, \quad (4)$$

where the remaining atoms are in the $q = 0$ momentum state. When a_{+q}^\dagger and a_{-q} act on $|\Psi_0\rangle$, terms with large occupation numbers j are enhanced: $a_{+q}^\dagger |n_{-q} = j, n_{+q} = j\rangle = \sqrt{j+1} |n_{-q} = j, n_{+q} = j+1\rangle$, $a_{-q} |n_{-q} = j, n_{+q} = j\rangle = \sqrt{j} |n_{-q} = j-1, n_{+q} = j\rangle$. In addition, $-q$ and $+q$ atoms occur only in pairs in the ground state. Together, these two effects cause both a_{+q}^\dagger and a_{-q} to increase the number of atoms in both the $-q$ and $+q$ states.

The experiments were performed with condensates of 3×10^7 sodium atoms in a magnetic trap with radial and axial trapping frequencies of 37 and 7 Hz, respectively [11]. The condensate had a peak density of $1.0 \times 10^{14} \text{ cm}^{-3}$ corresponding to a chemical potential of $\mu = h \times 1.5 \text{ kHz}$, a sound velocity of $c = 5 \text{ mm/s}$, and a Thomas-Fermi radial radius of $32 \mu\text{m}$. The Bragg beams for the optical lattices were generated from a common source of laser light 1.7 GHz red-detuned from the $3S_{1/2}|F=1\rangle$ to $3P_{3/2}|F'=0,1,2\rangle$ transitions. The lattices were moved radially through the cloud. This was done to avoid the high collisional density along the axial direction, where outcoupled atoms would have undergone elastic collisions with the condensate [12]. The Bragg beams for the optical lattices were generated from a common source of laser light 1.7 GHz red-detuned from the $3S_{1/2}|F=1\rangle$ to $3P_{3/2}|F'=0,1,2\rangle$ transitions. The lattices were moved radially through the cloud. This was done to avoid the high collisional density along the axial direction, where outcoupled atoms would have undergone elastic collisions with the condensate [12]. The Bragg beams for the optical lattices were generated from a common source of laser light 1.7 GHz red-detuned from the $3S_{1/2}|F=1\rangle$ to $3P_{3/2}|F'=0,1,2\rangle$ transitions. The lattices were moved radially through the cloud. This was done to avoid the high collisional density along the axial direction, where outcoupled atoms would have undergone elastic collisions with the condensate [12].

The momentum analysis of the phonons was performed with two counterpropagating beams that imparted a recoil momentum of $Q = m \times 59 \text{ mm/s}$ onto the outcoupled atoms. The beams were polarized parallel to the longitudinal axis of the condensate to suppress super-radiant emission [13]. A frequency difference (“probe frequency”) of 100 kHz between the two beams corresponded to the kinetic energy needed for atoms initially at rest to reach this recoil momentum. To gain recoil momentum $+Q$, atoms with initial momentum $+q$ were resonant at 107 kHz (Fig. 1a). Atoms with momentum $-q$ were reso-

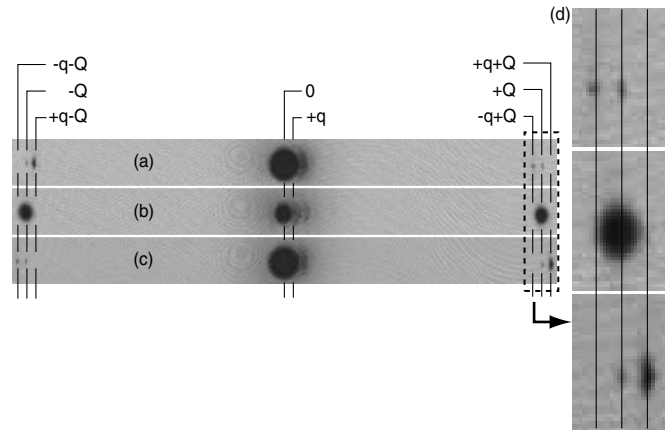


FIG. 1. Momentum distribution of a condensate with phonons. After imprinting $+q$ phonons into the condensate, momentum analysis via Bragg spectroscopy transfers a momentum $\pm Q$ (two-photon recoil) to the atoms. Absorption images after 40 ms time of flight in (a), (b), and (c) show the condensate in the center and outcoupled atoms to the right and left for probe frequencies of 94, 100, and 107 kHz, respectively. The small clouds centered at $+q$ are phonons that were converted to free particles. The size of the images is $25 \times 2.2 \text{ mm}$. (d) The outlined region in (a)–(c) is magnified, and clearly shows outcoupled atoms with momenta $Q \pm q$, implying that phonons with wave vector q/\hbar have both $+q$ and $-q$ free particle momentum components.

nant at 94 kHz (Fig. 1b). In our experiment, a retro-reflected beam containing both optical frequencies resulted in two optical lattices moving at the same speed in opposite directions. This led to simultaneous outcoupling of $+q$ and $-q$ atoms in opposite directions. These large-angle Bragg beams were pulsed on for 0.5 ms. The probe pulse had to be long enough to selectively excite atoms with $\pm q$ momentum, but also shorter than h/μ for the mean-field energy to be negligible during the readout. Each frequency component had an intensity of 0.7 mW/cm^2 , corresponding to a two-photon Rabi frequency of 700 Hz. Subsequently, the trap was turned off and a resonant absorption image was taken after 40 ms of ballistic expansion.

Figure 1 shows typical absorption images for various probe frequencies. The quasiparticle nature of the phonons was directly evident (see outlined region) in the time-of-flight distribution through the presence of the peaks at momenta $\pm q + Q$. These peaks had well-defined momentum because the outcoupled atoms left the condensate quickly (during this time the atoms’ velocity changed by less than the speed of sound [14]). This “photograph” of the Bogoliubov transformation is the central result of this paper.

We now discuss the different momentum components distinguishable in Fig. 1: (i) The original condensate is in the center. (ii) The condensate is asymmetrically extended towards positive momenta. This is due to imprinted phonons of momentum q that were converted to free particles during the ballistic expansion. Previously this signature was used to determine the structure factor of a condensate [6]. There is no momentum component in the

opposite direction, because we did not create $-q$ phonons (see below). The smearing of the observed momentum distribution may be caused by acceleration due to the inhomogeneous density distribution of the condensate when the trap was switched off. (iii) The two components with momentum $+Q$ and $-Q$ are atoms outcoupled from the condensate at rest. The symmetry of the $\pm Q$ peaks, as well as the position of the main condensate, served as an indicator as to whether the condensate was undergoing dipole oscillation during the experiment. Images that showed such “sloshing” (caused by technical noise) were excluded from further analysis. (iv) Atoms at $+q + Q$ (Fig. 1c) and $+q - Q$ (Fig. 1a) are coupled out from the $+q$ component of the phonons. (v) Atoms at $-q - Q$ (Fig. 1c) and $-q + Q$ (Fig. 1a) are coupled out from the $-q$ component of the phonons.

Quantitative information was obtained by scanning the probe frequency and measuring the number of outcoupled atoms in the three peaks around $-Q$ (See Fig. 1). Without phonons only the condensate peak is observed. The excitation of phonons at wave vector $+q$ creates momentum sidebands at momentum $\pm q$. The $-q$ peak is expected to be smaller by a factor v_q^2/u_q^2 . This effect is evident in Fig. 2, but with a poor signal-to-noise ratio.

The excitation of the phonons was characterized by scanning the frequency difference of the small-angle Bragg beams (Fig. 3a) and measuring the number of outcoupled atoms at $+q - Q$. The probe frequency was kept at 94 kHz because the momenta of the excited phonons remained fixed. The observation of two distinct peaks (corresponding to $+q$ at 400 Hz and $-q$ phonons at -400 Hz) confirms that there was sufficient resolution to excite only $+q$ phonons and suppress the off-resonant excitation of $-q$ phonons. The higher peak represents the u component of $+q$ phonons excited at positive excitation frequencies. When the excitation frequency became negative, $-q$

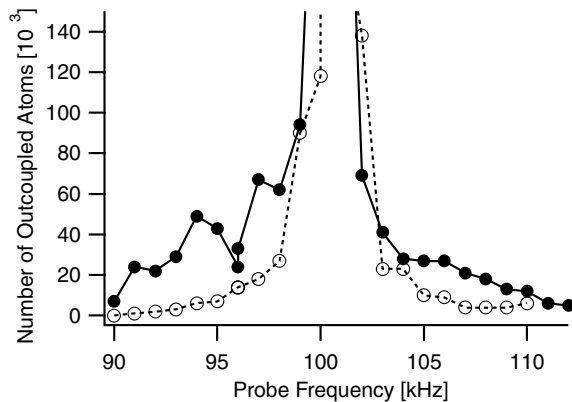


FIG. 2. Bragg spectrum of a condensate with (●) and without (○) phonon excitation. The number of outcoupled atoms vs the probe frequency is shown. The excitation of phonons creates sidebands on both sides of the central condensate peak. At about 100 kHz, the absorption images were saturated due to high optical density.

phonons were excited. This second peak represents the v component of the phonons.

According to Eq. (3) the ratio of the two peaks, v_q^2/u_q^2 , should be smaller at lower density. This is confirmed in Fig. 3b, which shows the excitation spectrum at low density. The density was lowered by a factor of 2 by weakening the axial trap frequency to 4 Hz and reducing the number of atoms in the condensate by a factor of 3. The scatter in the data could be due to residual sloshing, shot-to-shot fluctuations in the size of the condensate, or non-linear effects (see below).

The dashed line is the theoretical prediction with no free parameters (except the vertical scale). It was obtained by integrating Eq. (3) over the inhomogeneous density distribution of the condensate and by accounting for the finite length of the square excitation pulse, which broadens the line and causes the extra sidelobes at about 900 Hz. The theory assumes the validity of a perturbative approach, i.e., that the excitation pulse is weak.

Ideally, both Bragg pulses should affect only a few percent of the atoms, as in previous experiments [6,7].

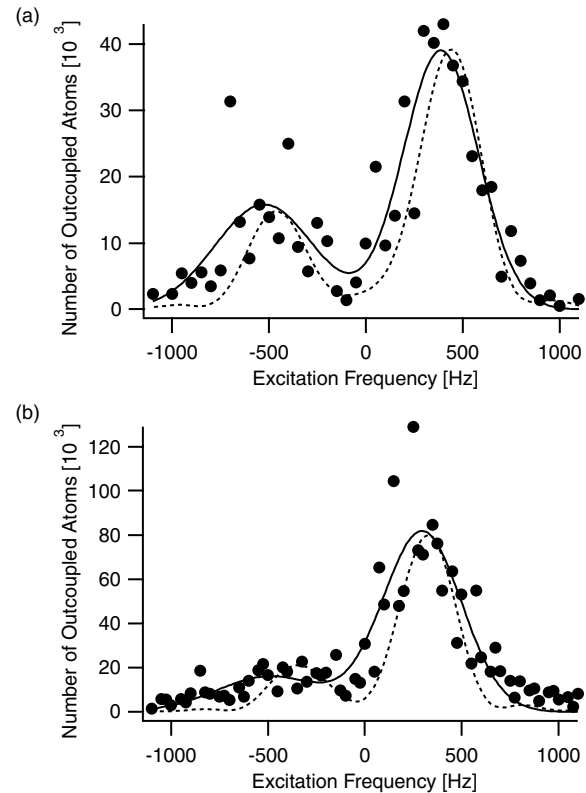


FIG. 3. Phonon excitation spectrum. Atoms with initial momentum $+q$ were detected by setting the probe frequency to 94 kHz and measuring the number of atoms with momentum $-Q + q$. The two peaks reflect that phonons with $+q/\hbar$ and $-q/\hbar$ wave vectors have free particle components with momentum $+q$. Spectra were taken at (a) high density ($1.0 \times 10^{14} \text{ cm}^{-3}$) and (b) low density ($0.5 \times 10^{14} \text{ cm}^{-3}$). The solid line, a fit to the sum of two Gaussians, is intended to guide the eye. The dashed line is the theoretical prediction.

However, because our signal was the product of the two outcoupling efficiencies, we needed to work at much higher outcoupled fractions. We estimate that the excitation pulse transferred 10% of the condensate atoms into the phonon state, and that the probe pulse outcoupled 40% of these atoms on resonance.

Both Bragg processes (stimulated Rayleigh scattering) should depend only on the product of the two intensities. Therefore, changing the sign of the excitation frequency should not affect the number of phonons generated (assuming a stationary condensate). However, when the sign of the excitation frequency was changed in our experiment, the observed number of phonons differed. This is most likely due to superradiance [13], which is sensitive to the individual intensities. Therefore, the asymmetry in phonon number was eliminated by ensuring equal intensities in the two beams. Additionally, there was a substantial loss ($\sim 50\%$) of condensate atoms due to superradiant Rayleigh scattering. Both superradiant effects could be further suppressed using light further detuned from resonance. However, in our case this would have required an additional laser. Given these experimental limitations, the agreement between experiment and theory in Fig. 3 is satisfactory.

In this work we have used large-angle Bragg pulses to analyze the momentum structure of the phonon wave function. In principle, this could have also been achieved by removing the mean-field interaction within a time $\hbar/\varepsilon(q)$ and then probing the velocity distribution of the particles. This is not possible with ordinary ballistic expansion because the reduction of the interactions is too slow, taking place on a time scale of the trapping period. However, the use of a Feshbach resonance [15] would provide an effective method for suddenly reducing the mean-field interaction.

In conclusion, we have experimentally analyzed the phonon wave function in a Bose-Einstein condensate. Following recent theoretical work [5], the two-component character of Bogoliubov quasiparticles was observed in the frequency domain (Fig. 2). In addition, the momentum components of the phonon wave function were discriminated by their final momenta after the probe pulse (Fig. 1). By combining momentum and frequency

selectivity, we were able to directly photograph the Bogoliubov transformation (Fig. 1d), demonstrating the power of Bragg spectroscopy to analyze nontrivial wave functions. This method may also be applicable to studying the many-body and vortex states [8] of dilute atomic Bose-Einstein condensates.

This work was funded by ONR, NSF, ARO, NASA, and the David and Lucile Packard Foundation. We are grateful to A. Brunello and S. Stringari for insightful discussions.

*Current address: School of Physics, Georgia Institute of Technology, Atlanta, Georgia 30332.

†Group website: http://cua.mit.edu/ketterle_group/

- [1] N. N. Bogoliubov, J. Phys. (USSR) **11**, 23 (1947).
- [2] A. Einstein, Sitzungsber. Preuss. Akad. Wiss. Bericht **3**, 18 (1925).
- [3] L. D. Landau, J. Phys. (USSR) **5**, 71 (1941).
- [4] N. Birell and P. Davies, *Quantum Fields in Curved Space* (Cambridge University Press, Cambridge, UK, 1982).
- [5] A. Brunello, F. Dalfovo, L. Pitaevskii, and S. Stringari, Phys. Rev. Lett. **85**, 4422 (2000).
- [6] D. M. Stamper-Kurn, A. P. Chikkatur, A. Görlitz, S. Inouye, S. Gupta, D. E. Pritchard, and W. Ketterle, Phys. Rev. Lett. **83**, 2876 (1999).
- [7] J. Stenger, S. Inouye, A. P. Chikkatur, D. M. Stamper-Kurn, D. E. Pritchard, and W. Ketterle, Phys. Rev. Lett. **82**, 4569 (1999).
- [8] F. Zambelli, L. Pitaevskii, D. M. Stamper-Kurn, and S. Stringari, Phys. Rev. A **61**, 063608 (2000).
- [9] P. B. Blakie, R. J. Ballagh, and C. W. Gardiner, cond-mat/0108480.
- [10] K. Huang, *Statistical Mechanics* (Wiley, New York, 1987).
- [11] R. Onofrio, D. S. Durfee, C. Raman, M. Köhl, C. E. Kulewicz, and W. Ketterle, Phys. Rev. Lett. **84**, 810 (2000).
- [12] A. P. Chikkatur, A. Görlitz, D. M. Stamper-Kurn, S. Inouye, S. Gupta, and W. Ketterle, Phys. Rev. Lett. **85**, 483 (2000).
- [13] S. Inouye, A. P. Chikkatur, D. M. Stamper-Kurn, J. Stenger, D. E. Pritchard, and W. Ketterle, Science **285**, 571 (1999).
- [14] E. W. Hagley, L. Deng, M. Kozuma, J. Wen, K. Helmerson, S. L. Rolston, and W. D. Phillips, Science **283**, 1706 (1999).
- [15] S. Inouye, M. R. Andrews, J. Stenger, H.-J. Miesner, D. M. Stamper-Kurn, and W. Ketterle, Nature (London) **392**, 151 (1998).